# High-repetition-rate near-infrared noncollinear ultrabroadband optical parametric amplification in $KTiOPO_4$

**Oleksandr Isaienko,[1,2] Eric Borguet,[2,3] and Peter Vöhringer[1,4]**

[1]*Institut für Physikalische und Theoretische Chemie, Rheinische Friedrich-Wilhelms-Universität, Wegelerstrasse 12, Bonn, 53115, Germany*

[2]*Chemistry Department, Temple University, 1901 N. 13th Street, Philadelphia, Pennsylvania, 19122, USA*

[3]*e-mail: eborguet@temple.edu*

[4]*e-mail: p.voehringer@uni-bonn.de*

Received July 1, 2010; revised October 7, 2010; accepted October 14, 2010; posted October 15, 2010 (Doc. ID 130994); published November 11, 2010

We report efficient noncollinear optical parametric amplification (NOPA) of ultrabroadband near-IR pulses tunable in the 1.1–1.5 $\mu$m range at a repetition rate of 250 kHz. Improved generation of smooth near-IR continua (extending over ~1.0–1.6 $\mu$m) at 250 kHz was achieved by weakly focusing ~20% of the 1 W driving laser beam into a sapphire plate with longer focal length lenses than previously reported. Using bulk potassium-titanyl phosphate ($KTiOPO_4$) pumped at 800 nm, powers as high as 11 mW (14% pump conversion efficiency) and signal pulse durations as short as 23 fs were obtained after a single white-light seeded NOPA stage. 

*OCIS codes:* 190.4410, 190.4970, 320.7110.

The generation of intense ultrashort pulses in the near- and mid-IR is becoming increasingly important for a vast range of applications, including telecommunications, ultrafast spectroscopies, and high-harmonic generation. Noncollinear optical parametric amplification (NOPA) has become an efficient tool for the generation of such pulses [1] and was recently extended to the near-IR wavelength range (~1–2 $\mu$m) [2–5]. In these studies, the NOPAs operate at a repetition rate of 1 kHz, typical for the high-energy chirped-pulse amplifiers that drive the devices. However, for many applications, higher repetition rates are desired to enable faster data acquisition combined with superior signal-to-noise ratios. Previously, it was shown that NOPA can be realized in the visible range (~500–900 nm) at repetition rates as high as 2 MHz using $\beta$-barium borate (BBO) [6–9] with pump-to-signal conversion efficiencies ranging from ~6%–7% [7] to ~30% [6,8].

Additionally, there has been significant progress in the generation of high-repetition-rate tunable femtosecond pulses in the near- and mid-IR [10–13]. Recently, optical parametric chirped-pulse amplification (OPCPA) of microjoule-energy ~100 fs pulses at 3.3–3.7 $\mu$m at 100 kHz was reported [11,12]. Efficient optical parametric generation/amplification of near-IR pulses has been demonstrated by directly pumping periodically poled lithium niobate with a 1 MHz Yb-based oscillator with a peak internal efficiency of ~30% [13]. However, such systems were mostly designed for collinear phase matching, which normally limits the bandwidth and, consequently, the minimum attainable pulse durations to ~50–70 fs. Most recently [14], collinear-geometry OPCPA in aperiodically poled MgO:$LiNbO_3$ has been demonstrated to generate broadband ~3.5 $\mu$m microjoule pulses at 100 kHz; however, careful engineering of such nonlinear optical materials is required. To our knowledge, the amplification of high-repetition-rate IR broadband pulses in a noncollinear geometry has not been fully explored. In addition, data on the generation of near-IR seed pulses via self-phase modulation at very high repetition rates are scarce, and the reported spectra [7,15] of the white-light continua (WLC) were limited to wavelengths below ~1.2 $\mu$m. Motivated by recent progress in broadband near-IR generation at lower repetition rates, as well as by a study of near-IR continuum generation in various laser host materials at 1 kHz [16], we explored the feasibility of few-cycle pulse generation in this important spectral region at pulse repetition periods below 10 $\mu$s. To this end, a near-IR NOPA based on bulk potassium-titanyl phosphate ($KTiOPO_4$, KTP) was designed that was optimized for operation at a repetition rate as high as 250 kHz.

The pump source for the near-IR NOPA was a Coherent RegA 9050 laser that provides ~55 fs, 800 nm pulses with >4 $\mu$J/pulse energies at repetition rates of up to

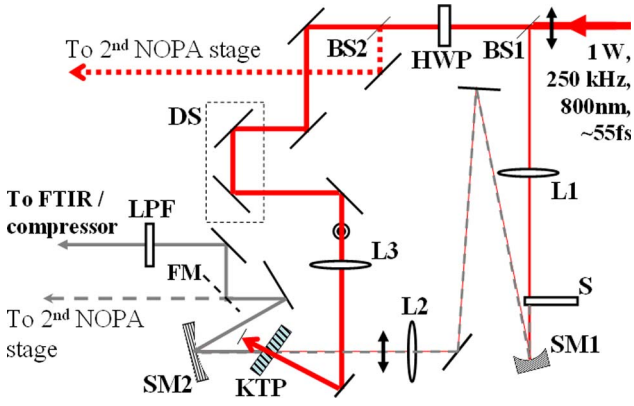


Fig. 1. (Color online) Optical setup of the 250 kHz NOPA: KTP, 2 mm thick uncoated crystal (cut at $\theta = 42°$, $\varphi = 0°$ for phase matching in the $x$–$z$ plane); HWP, half-wave plate; BS1, BS2, beam splitters; L, lenses (L1, BK7, $f = 80$ mm; L2, quartz, 250 mm; L3, BK7, 300 mm); S, 2 mm thick sapphire plate; DS, delay stages; SM, silver spherical mirrors (SM1, $f = 25$ mm; SM2, 200 mm); FM, flipping mirror; LPF, long-pass near-IR filter RG-1000. Double-headed arrows and dotted circles indicate the polarization of 800 nm beam.

 

250 kHz (Fig. 1) [17]. Broadband near-IR seed pulses were generated by focusing a portion of the RegA's output into a 2 mm sapphire substrate. Following recent findings on improved IR continuum generation in laser host materials [16], we also tested a 4-mm-thick YAG plate using identical focusing conditions as for sapphire. In stark contrast to the sapphire substrate, the resultant near-IR WLC from YAG (not shown here) were strongly modulated, which in turn led to a spectrally deteriorated output from the KTP-NOPA. We therefore preferred sapphire for white-light seeding.

Several conditions were tested for near-IR continuum generation, including the use of lenses with different focal lengths. The resultant WLC was collimated by a spherical mirror and imaged onto a Bruker Vertex Fourier transform IR (FTIR) spectrometer equipped with a liquid $N_2$ cooled HgCdTe detector. A comparison of spectra of the 800 nm fundamental that were independently acquired with the Vertex and a REES spectrum analyzer confirmed the excellent reliability of the FTIR data. In Fig. 2, white-light spectra for three representative focal lengths are plotted semilogarithmically as a function of wavelength, $\lambda$. All spectra exhibit an exponentially decaying near-IR tail that can be used for seeding the subsequent NOPA stage. The quality of the WLC is specified reliably by the slope, $\mathrm{d}(\log I)/\mathrm{d}\lambda$. At a driving power of 200 mW (~0.8 $\mu$J/pulse), a focal length of 80 mm yielded the broadest spectrum with a minimal slope of $3.13 \times 10^{-3}$ nm$^{-1}$, thus generating a WLC with a much better quality than those generated at conventional repetition rates of 1 kHz [16]. The much improved quality of the near-IR WLC when using a longer focal length lens is in accord with a recent report of continuum generation in various laser host materials [16]. We believe this effect is related to the prevalence of self-focusing over external focusing during continuum generation in the low NA regime, as previously suggested for broadening of the high-frequency wing of WLC generated from fused silica [18]. In particular, it was found that, for NA < 0.05, the broadening effect is largest, while the threshold for continuum generation is low (0.3–0.4 $\mu$J) [18]. In the WLC arm (Fig. 1), focusing is even weaker (NA ~ 0.018), which may assist in broadening the Stokes wing of the WLC.

For parametric amplification of the WLC, a beam splitter (BS2, reflectivity ~30% for *s*-polarization) was used to divide the remaining fundamental of the front end (~3.2 $\mu$J/pulse) into two beams, whose polarization was adjusted with a half-wave plate in front of BS2 (Fig. 1). The lower-energy beam was sent to pump the KTP crystal and was slightly attenuated for better control of focusing conditions (the higher-energy beam serves to pump a second NOPA stage whose performance is currently being characterized). The near-IR white-light beam was overlapped with ~110 mW of the 800 nm pump beam in KTP, and several internal signal–pump angles around 3°–4° were tested [5,19]. The pump was focused with a 300 mm BK7 lens placed ~330 mm before the crystal (pump peak intensity ~10 GW/cm$^2$ at the crystal [17]). Such loose focusing was used to preserve the good spatial quality of the amplified near-IR beam. The tuning of signal pulses was achieved by changing the phase-matching angle between the pump beam and the $z$ axis of the KTP crystal. A flipping mirror after KTP allowed for steering the IR signal pulses either into the FTIR spectrometer for spectral characterization or into a prism compressor for group-velocity dispersion compensation. Temporal characterization of the compressed pulses was carried out by measuring second-order interferometric autocorrelations in a 100-$\mu$m-thick BBO crystal.

Typical spectra of the signal pulses after the KTP-NOPA stage are shown in Fig. 3 for an internal noncollinear angle between the signal and the pump of 3.8°. The achieved output power of the signal pulses is plotted in the upper panel as a function of the calculated center-of-mass wavelength. The spectral FWHM of the amplified signal pulses varies between more than 1100 cm$^{-1}$ to somewhat below 500 cm$^{-1}$ as the NOPA is tuned toward longer wavelengths. The spectra are not as broad as those obtained previously at 1 kHz [5,19]. However, they support transform-limited pulse durations ranging between 15 and 35 fs. The resultant power of the signal beam at the peak of the tuning curve (~11 mW, or ~44 nJ/pulse; Fig. 3) corresponds to a pump-to-signal conversion efficiency of ~10% and to an estimated total conversion efficiency (signal + idler) of ~14% after one pass.

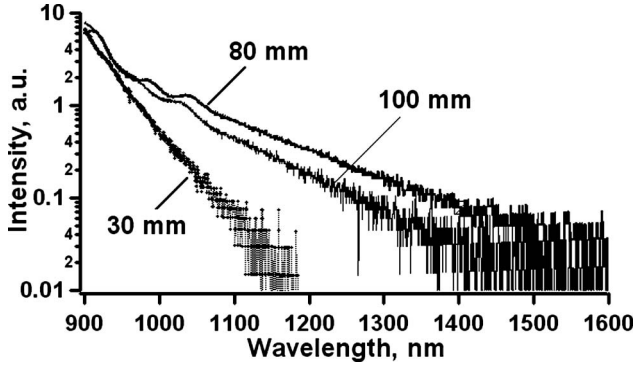


Fig. 2. Near-IR portion of the WLC obtained with different focal length lenses for imaging a pump beam into a 2 mm sapphire plate. The onset of digital noise at longer wavelengths reflects the limited dynamic range of the FTIR spectrometer. All spectra have been corrected for detector sensitivity, the RG-1000 filter transmission, and the finite frequency resolution of the FTIR spectrometer.

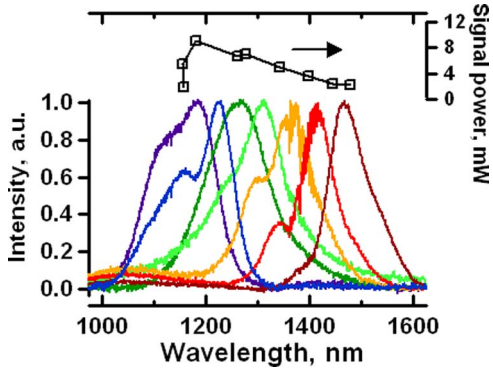


Fig. 3. (Color online) Normalized spectra of amplified signal pulses at various phase-matching angles of the pump beam after the KTP crystal (internal noncollinear angle of ~3.8°). The fine structures around 1400 nm are due to the water vapor overtone absorptions. Upper graph, signal beam power versus corresponding center-of-mass wavelengths (solid curve connects the data points).

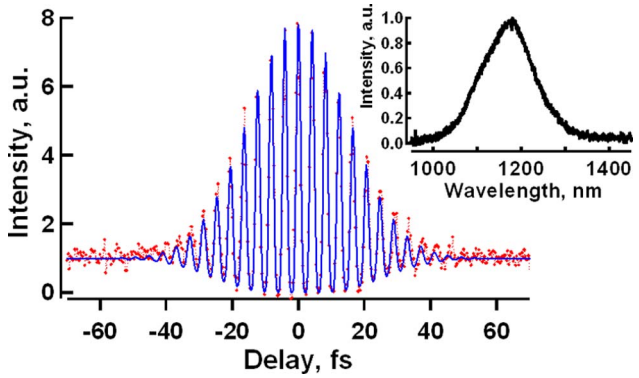


Fig. 4. (Color online) Interferometric autocorrelation of the compressed signal pulses coming from the KTP together with a Gaussian fit. The inset shows the power spectrum of the pulses.

As deduced from interferometric autocorrelations, the temporal width of the signal pulses directly after the NOPA decreased from ~69 to ~55 fs as their center wavelength was tuned from ~1200 to ~1400 nm. The compressibility of these amplified pulses was assessed at the maximum of the tuning curve and a noncollinear signal–pump angle of 3.8° (spectra in Fig. 3). At optimal compression, the apex distance between the two Suprasil prisms was 29 cm, corresponding to a group-delay dispersion (GDD) of –228 $fs^2$. The prism pair compensates almost completely the total calculated GDD of ~242 $fs^2$ at 1175 nm experienced by the near-IR signal as it travels through the sapphire plate (31 $fs^2$), the quartz lens L2 (16 $fs^2$), and the KTP crystal (195 $fs^2$). An interferometric autocorrelation of the compressed pulses is reproduced in Fig. 4, together with a simulation for a pulse having a Gaussian temporal profile with a width of 23 fs (FWHM). From the power spectrum measured simultaneously (Fig. 4, inset), a time–bandwidth product of 0.72 can be deduced corresponding to ~1.5× the transform limit.

In conclusion, we have demonstrated efficient near-IR NOPA in bulk KTP at repetition rates as high as 250 kHz. The NOPA described here is readily tunable throughout the range of ~1100–1550 nm with pulse energies up to 44 nJ after a single pass and pulse durations shorter than 25 fs. Although the postamplifier is still under full characterization, our preliminary results demonstrate that total signal + idler conversion efficiencies as high as 20% can be achieved in a dual stage design. We also envision our high-repetition-rate near-IR NOPA to soon become a powerful seed source (at ~1.0–1.1 $\mu$m) for further parametric amplification schemes, thereby paving the way to few-cycle mid-IR (~3–5 $\mu$m) pulse generation in nonlinear optical materials, such as those used in low-repetition-rate systems [20].

We greatly appreciate financial support from the German Academic Exchange Service, DAAD award A/08/79504, the Deutsche Forschungsgemeinschaft (DFG) through the SFB 813 “Chemistry at Spin Centers,” and the U.S. National Science Foundation (NSF) (NSF grant CHE 0809838). Acknowledgment is made to the donors of the American Chemical Society Petroleum Research Fund for support of this research.

## References

1. G. Cerullo and S. De Silvestri, Rev. Sci. Instrum. **74**, 1 (2003).
2. D. Brida, C. Manzoni, G. Cirmi, M. Marangoni, S. Bonora, P. Villoresi, S. De Silvestri, and G. Cerullo, J. Opt. A **12**, 013001 (2010).
3. D. Kraemer, R. Hua, M. L. Cowan, K. Franjic, and R. J. D. Miller, Opt. Lett. **31**, 981 (2006).
4. D. Brida, S. Bonora, C. Manzoni, M. Marangoni, P. Villoresi, S. De Silvestri, and G. Cerullo, Opt. Express **17**, 12510 (2009).
5. O. Isaienko and E. Borguet, Opt. Express **16**, 3949 (2008).
6. J. Piel, E. Riedle, L. Gundlach, R. Ernstorfer, and R. Eichberger, Opt. Lett. **31**, 1289 (2006).
7. A. Killi, A. Steinmann, G. Palmer, U. Morgner, H. Bartelt, and J. Kobelke, Opt. Lett. **31**, 125 (2006).
8. C. Schriever, S. Lochbrunner, P. Krok, and E. Riedle, Opt. Lett. **33**, 192 (2008).
9. J. Rothhardt, S. Hadrich, D. N. Schimpf, J. Limpert, and A. Tunnermann, Opt. Express **15**, 16729 (2007).
10. B. Golubovic and M. K. Reed, Opt. Lett. **23**, 1760 (1998).
11. C. Erny, C. Heese, M. Haag, L. Gallmann, and U. Keller, Opt. Express **17**, 1340 (2009).
12. O. Chalus, P. K. Bates, M. Smolarski, and J. Biegert, Opt. Express **17**, 3587 (2009).
13. M. Marangoni, R. Osellame, R. Ramponi, G. Cerullo, A. Steinmann, and U. Morgner, Opt. Lett. **32**, 1489 (2007).
14. C. Heese, C. R. Phillips, L. Gallmann, M. M. Fejer, and U. Keller, Opt. Lett. **35**, 2340 (2010).
15. M. K. Reed and M. K. S. Shepard, IEEE J. Quantum Electron. **32**, 1273 (1996).
16. M. Bradler, P. Baum, and E. Riedle, Appl. Phys. B **97**, 561 (2009).
17. M. K. Reed, M. K. Steiner-Shepard, and D. K. Negus, Opt. Lett. **19**, 1855 (1994).
18. J. B. Ashcom, R. R. Gattass, C. B. Schaffer, and E. Mazur, J. Opt. Soc. Am. B **23**, 2317 (2006).
19. O. Isaienko and E. Borguet, J. Opt. Soc. Am. B **26**, 965 (2009).
20. D. Brida, C. Manzoni, G. Cirmi, M. Marangoni, S. De Silvestri, and G. Cerullo, Opt. Express **15**, 15035 (2007).